Dynamical Analysis of Hydrological Indexes Extracted from Remote Sensing Imagery: An Introductory Study

Ivan E. Villalon-Turrubiates*
*Department of Telecommunications, Center of Research and Advanced Studies (CINVESTAV), Campus Guadalajara, Avenida Científica 1145, Colonia El Bajío, 45010, Zapopan Jalisco, México, Email: villalon@gdl.cinvestav.mx

Abstract — A new intelligent computational paradigm based on filtering techniques modified to enhance the quality of reconstruction of the physical characteristics of environmental electronic maps extracted from the large scale remote sensing imagery is proposed. First, the problem-oriented modification of the previously proposed fused Bayesian-regularization enhanced radar imaging method is performed to enable it to reconstruct remote sensing signatures of interest. Second, the extraction of the so-called hydrological electronic maps and the analysis of its dynamics are proposed. Finally, simulation results of hydrological remote sensing signatures reconstruction from enhanced real-world environmental images are reported to verify the efficiency of the proposed approach.

I. Introduction

Modern applied theory of reconstructive image processing is now a mature and well developed research field, presented and detailed in many works (see, for example [1] thru [11] and references therein). Although the existing theory offers a manifold of statistical and descriptive regularization techniques for reconstructive imaging in many application areas there still remain some unresolved crucial theoretical and processing problems related to large scale sensor array real-time reconstructive image processing.

In this study, we consider the problem of enhanced remote sensing (RS) imaging and reconstruction of remote sensing signature (RSS) fields of the RS scenes with the use of array radars or synthetic aperture radars (SAR) as sensor systems. Two principal developments constitute the major innovative contributions of this study, namely:

1) The development of a robust version of the fused Bayesian-regularization (FBR) method [1] for reconstruction of the power spatial spectrum pattern (SSP) of the wavefield scattered from the RS scene and related RSS given a finite set of SAR signal recordings. Since this is in essence a nonlinear numerical inverse problem, the ill-poseness problem can be alleviated via the robustification of the Bayesian estimation strategy [2], [3] by performing the non adaptive approximations of the SSP and RSS reconstructive operators that incorporate the non trivial metrics considerations for designing the proper solution space and different regularization constraints imposed on a solution.

2) The development of a new robust filtering method that provides the possibility to track, filter and predict the dynamical behavior of the physical characteristics extracted from the real-world RS imaging provided with the use of segmentation and classification methodologies for feature extraction to generate the so-called hydrological electronic maps (HEM).

II. Problem Model

Consider the measurement data wavefield $u(\mathbf{y})=s(\mathbf{y})+n(\mathbf{y})$ modeled as a superposition of the echo signals s and additive noise n that assumed to be available for observations and recordings within the prescribed time-space observation domain $Y \ni \mathbf{y}$. The model of observation wavefield u is specified by the linear stochastic equation of observation (EO) of operator form [1] as $u=Se+n$ ($e \in \mathrm{E}$; $u,n \in \mathrm{U}$; $S:\mathrm{E}\to\mathrm{U}$) in the L_2 Hilbert signal spaces E and U [1] with the metric structures induced by inner products,

$$[e_1,e_2]_{\mathrm{E}}=\int_{F\times X} e_1(f,\mathbf{x})e_2^*(f,\mathbf{x})df d\mathbf{x}\,,$$
$$[u_1,u_2]_{\mathrm{U}}=\int_{Y} u_1(\mathbf{y})u_2^*(\mathbf{y})d\mathbf{y}\,, \tag{1}$$

respectively, where * stands for complex conjugate. The operator model of the stochastic EO in the conventional integral form may be rewritten as [1]

$$u(\mathbf{y})=\int_{F\times X} S(\mathbf{y},\mathbf{x})e(f,\mathbf{x})df d\mathbf{x}+n(\mathbf{y})\,,$$
$$e(f,\mathbf{x})=\int_{T} \varepsilon(t;\mathbf{x})\exp(-j2\pi ft)dt\,, \tag{2}$$

where $\varepsilon(t;\mathbf{x})$ represents the stochastic backscattered wavefield fluctuating in time t, and the functional kernel $S(\mathbf{y},\mathbf{x})$ of the signal formation operator (SFO) S in Eq. (2) is specified by the particular employed RS signal wavefield formation model [4]. The phasor $e(f,\mathbf{x})$ in Eq. (2) represents the backscattered wavefield $e(f)$ over the frequency-space observation domain $F\times P\times\Theta$ [1], in the slant range $\boldsymbol{\rho}\in P$ and azimuth angle $\boldsymbol{\theta}\in\Theta$ domains, $\mathbf{x}=(\boldsymbol{\rho},\boldsymbol{\theta})^{\mathrm{T}}$, $\mathbf{X}=P\times\Theta$, respectively. The RS imaging problem is to find an estimate $\hat{B}(\mathbf{x})$ of the power SSP $B(\mathbf{x})$ [2], [3] in the $X \ni \mathbf{x}$ environment via processing whatever values of measurements of the data wavefield $u(\mathbf{y})$, $\mathbf{y}\in Y$ are available.

Following the RS methodology [1], any particular physical RSS of interest is to be extracted from the reconstructed RS image $\hat{B}(\mathbf{x})$ applying the so-called signature extraction operator Λ [5]. The particular RSS is mapped applying Λ to the reconstructed image, i.e.

$$\hat{\Lambda}(\mathbf{x}) = \Lambda(\hat{B}(\mathbf{x})) . \quad (3)$$

Taking into account the RSS extraction model of Eq. (3), the signature reconstruction problem is formulated as follows: to map the reconstructed particular RSS of interest $\hat{\Lambda}(\mathbf{x}) = \Lambda(\hat{B}(\mathbf{x}))$ over the observation scene X∋**x** via post-processing Eq. (3) whatever values of the reconstructed scene image $\hat{B}(\mathbf{x})$, $\mathbf{x}\in X$ are available. The experiment design (ED) considerations for inducing the metrics structure in the solution space are defined by the inner product [1]

$$\|\mathbf{B}\|^2_{B(K)}=[\mathbf{B},\mathbf{MB}] , \quad (4)$$

where **M** is referred to as the metrics inducing operator [1]. Hence, the selection of **M** provides additional geometrical degrees of freedom of the problem model. The model of **M** incorporated corresponds to a matrix-form approximation of the Tikhonov's stabilizer of the second order that was numerically designed in [1]. Also, following [1] the projection-type a priori information incorporated requires that the SSP vector **B** satisfies the linear constraint equation

$$\mathbf{GB}=\mathbf{C} , \text{ i.e. } \mathbf{G}^{-}\mathbf{GB}=\mathbf{B}_P , \quad (5)$$

where $\mathbf{B}_P=\mathbf{G}^{-}\mathbf{C}$ and $\mathbf{G}^{-}$ is the Moore-Penrose pseudoinverse of a given constraint operator $\mathbf{G}:B_{(K)}\rightarrow B_{(Q)}$ [1], and the constraint vector $\mathbf{C}\in B_{(Q)}$ and the constraint subspace $B_{(Q)}$ (Q<K) are assumed to be given. In Eq. (5), the constraint operator **G** projects the portion of the unknown SSP onto the subspace where the SSP values are fixed by **C**.

The algorithmic-level purpose is to develop a generalization of the FBR estimator [2], [3] for the problem of high-resolution RSS reconstruction incorporating the descriptive robustification of the fused Bayesian-regularization technique (RFBR) to alleviate the problem ill-poseness.

III. Generalization of the FBR Method

The estimator that produces the optimal estimate $\hat{\mathbf{B}}$ of the SSP vector applying the FBR estimation strategy that incorporates nontrivial a priori geometrical and projection-type model information [2], [3] was developed in a previous study [1]. Such optimal FBR estimate of the SSP is given by the nonlinear equation [1]

$$\hat{\mathbf{B}} =\mathbf{B}_P+\mathbf{PB}_0+\mathbf{W}(\hat{\mathbf{B}})(\mathbf{V}(\hat{\mathbf{B}})-\mathbf{Z}(\hat{\mathbf{B}})) . \quad (6)$$

In Eq. (6), $\mathbf{B}_P$ is defined by Eq. (5) and $\mathbf{B}_0$ represents the a priori SSP distribution to be considered as a zero step approximation to the desires SSP $\hat{\mathbf{B}}$. The sufficient statistics (SS) vector is $\mathbf{V}(\hat{\mathbf{B}})=\{\mathbf{F}(\hat{\mathbf{B}})\mathbf{U}\mathbf{U}^{+}\mathbf{F}^{+}(\hat{\mathbf{B}})\}_{diag}$ ($\{\cdot\}_{diag}$ defines a vector composed of the principal diagonal of the embraced matrix), the solution-dependent SS formation operator

$$\mathbf{F}=\mathbf{F}(\hat{\mathbf{B}})=\mathbf{D}(\hat{\mathbf{B}})(\mathbf{I}+\mathbf{S}^{+}\mathbf{R}_N^{-1}\mathbf{SD}(\hat{\mathbf{B}}))^{-1}\mathbf{S}^{+}\mathbf{R}_N^{-1} , \quad (7)$$

the SS shift vector $\mathbf{Z}(\hat{\mathbf{B}})=\{\mathbf{F}(\hat{\mathbf{B}})\mathbf{R}_N\mathbf{F}^{+}(\hat{\mathbf{B}})\}_{diag}$ [1], and the composite solution-dependent smoothing-projection window operator [1] is defined as

$$\mathbf{W}(\hat{\mathbf{B}})=\mathbf{P}\boldsymbol{\Omega}(\hat{\mathbf{B}}) \quad (8)$$

with the projector

$$\mathbf{P}=(\mathbf{I}-\mathbf{G}^{-}\mathbf{G}) \quad (9)$$

and the solution-dependent regularizing window

$$\boldsymbol{\Omega}(\hat{\mathbf{B}})=(\mathrm{diag}(\{\mathbf{S}^{+}\mathbf{F}^{+}\mathbf{FS}\}_{diag})+\alpha\mathbf{D}^2(\hat{\mathbf{B}})\mathbf{M}(\hat{\mathbf{B}}))^{-1} , \quad (10)$$

in which the regularization parameter α is to be adaptively adjusted using the system calibration data from Eq. (5). The generalization of the FBR estimator of Eq. (6) for the case of RSS reconstruction can now be performed as [2], [3]

$$\hat{\Lambda}_{(K)}(\mathbf{x}) = \sum_{k=1}^{K}\Lambda(\hat{B}_k)\,|g_k(\mathbf{x})|^2 . \quad (11)$$

Hence, in the adapted pixel-format solution space, the vector $\hat{\Lambda} = \Lambda(\hat{B})$ composed of pixels $\{\Lambda(\hat{B}_k);k=1,\ldots,K\}$ represents the desired pixel-format map of the high-resolution RSS reconstructed over the observed scene.

Because of the complexity of the solution-dependent operator inversions needed to be performed to compute the SS, the computational complexity of such generalized optimal algorithm of Eq. (11) is extremely high. Hence, Eq. (11) could not be addressed as a practically realizable estimator of the RSS.

IV. RFBR Technique for RSS Reconstruction

The robustification scheme for implementation of the generalized FBR estimator reduces drastically the computation load of the RSS formation procedure from Eq. (11) without substantial degradation in the SSP resolution and overall RSS map performances, via roughing **P**=**I** and performing the robustification (nonadaptive approximation) of both the SS formation operator $\mathbf{F}(\hat{\mathbf{B}})$ and the smoothing window $\boldsymbol{\Omega}(\hat{\mathbf{B}})$ in Eq. (6) by roughing $\mathbf{D}(\hat{\mathbf{B}})\approx\mathbf{D}=\beta\mathbf{I}$, where β represents the expected a priori image gray level [1]. Thus, the robust SS formation operator

$$\mathbf{F}=\mathbf{A}^{-1}(\rho)\mathbf{S}^{+} \text{ with } \mathbf{A}(\rho)=\mathbf{S}^{+}\mathbf{S}+\rho^{-1}\mathbf{I} \quad (12)$$

becomes a regularized inverse of the SFO **S** with regularization parameter ρ^{-1}, the inverse of the signal-to-noise ratio (SNR) $\rho=\beta/N_0$ for the adopted white observation noise model, $\mathbf{R}_N=N_0\mathbf{I}$. The robust smoothing window

$$\mathbf{W}=\boldsymbol{\Omega}=(w_0\mathbf{I}+\mathbf{M})^{-1} \quad (13)$$

is completely defined now by matrix **M** that induces the metrics structure from Eq. (4) in the solution space with the scaling factor $w_0=\mathrm{tr}\{\mathbf{S}^{+}\mathbf{F}^{+}\mathbf{FS}\}/K$ [1]. The resulting RFBR estimator is defined as [2], [3]

$$\hat{\Lambda}_{RFBR}(\mathbf{x})=\mathbf{g}^{T}(\mathbf{x})\mathrm{diag}(\Lambda(\mathbf{B}_0+\boldsymbol{\Omega}\mathbf{V}))\mathbf{g}(\mathbf{x}) \quad (14)$$

where $\mathbf{V}=\{\mathbf{FUU}^{+}\mathbf{F}^{+}\}_{diag}$ represents the robust SS vector. Thus, the principal computational load of the RFBR estimator of Eq. (14) is associated now with the operator inversions required to compute the solution operator of Eq. (13) for adaptively (recurrently) adjusted regularization parameter ρ^{-1}.

V. RSS Segmentation and Classification

For this particular study, covered water, humid and dry zones are analyzed as particular RSS of interest. We consider the HEMs extracted via fusion of the weighted order statistics (WOS) method [6] with the minimum distance to mean (MDM) methodology [7].

The WOS is a methodology that can be considered as a generalization of the median filtering, where the information of all the order statistics is combined to provide an improved estimate of a variable [6].

The MDM decision rule is based on minimum distance classification of the mean values of a given set of pixels [7].

The fused WOS-MDM algorithm provide an accurate segmentation and classification for a particular physical index extracted from the reconstructed RSS.

VI. Dynamic RSS Reconstruction

The crucial issue in application of the modern dynamic filter theory to the problem of reconstruction of the desired RRS in current time is related to modeling of the RSS as a random field (spatial map developing in evolution time) that satisfies the dynamical difference state equation [8], [9] described as follows

$$\mathbf{z}(i+1) = \mathbf{\Phi}(i)\mathbf{z}(i) + \mathbf{\Gamma}(i)\mathbf{x}(i), \quad \mathbf{\Lambda}(i) = \mathbf{C}(i)\mathbf{z}(i), \tag{15}$$

and specified by the linear dynamic model formation operators (matrices) $\mathbf{\Phi}(i)$, $\mathbf{\Gamma}(i)$ and $\mathbf{C}(i)$, respectively [9]. The dynamical estimation strategy for such optimal RSS prediction procedure can now be defined as follows

$$\hat{\mathbf{z}}(i+1) = \left\langle \mathbf{z}(i+1) \middle| \hat{\mathbf{z}}(i); \hat{\mathbf{B}}(i+1) \right\rangle = \left\langle \mathbf{z}(i+1) \middle| \hat{\mathbf{B}}(i+1); \mathbf{m}_{\mathbf{z}}(i+1) \right\rangle, \tag{16}$$

routinely solving the dynamical RSS filtration problem of Eq. (16) for the current $(i+1)$st discrete-time prediction-estimation step, the desired technique becomes

$$\hat{\mathbf{z}} = \mathbf{m}_{\mathbf{z}}(i+1) + \mathbf{\Sigma}(i+1)\left[\hat{\mathbf{B}}(i+1) - \mathbf{H}(i+1)\mathbf{m}_{\mathbf{z}}(i+1)\right] \tag{17}$$

where $\mathbf{m}_{\mathbf{z}}(i+1)$ represents the predicted mean vector and the optimal dynamic filter operator $\mathbf{\Sigma}(i+1)$ is defined as

$$\begin{aligned} \mathbf{\Sigma}(i+1) &= \mathbf{K}_{\mathbf{\Sigma}}(i+1)\mathbf{H}^{T}(i+1)\mathbf{P}_{\mathbf{v}}^{-1}(i+1), \\ \mathbf{K}_{\mathbf{\Sigma}}(i+1) &= \left[\mathbf{\Psi}_{\mathbf{\Sigma}}(i+1) + \mathbf{P}_{\mathbf{z}}^{-1}(i+1)\right]^{-1}, \\ \mathbf{\Psi}_{\mathbf{\Sigma}}(i+1) &= \mathbf{H}^{T}(i+1)\mathbf{P}_{\mathbf{v}}^{-1}(i+1)\mathbf{H}(i+1). \end{aligned} \tag{18}$$

Last, using the derived filter Eq. (16) and Eq. (17), and the initial RSS state model given by (15), the optimal filtering procedure for dynamic reconstruction of the desired RSS map in the evolution discrete time [8], [9] becomes

$$\hat{\mathbf{\Lambda}} = \mathbf{\Phi}(i)\hat{\mathbf{z}}(i) + \mathbf{\Sigma}(i+1)\left[\hat{\mathbf{B}}(i+1) - \mathbf{H}(i+1)\mathbf{\Phi}(i)\hat{\mathbf{z}}(i)\right] \tag{19}$$

with the initial condition $\hat{\mathbf{\Lambda}}(0) = \Lambda\{\hat{\mathbf{B}}(0)\}$. The crucial issue to note here is related to model uncertainties regarding the particular employed dynamical RSS model of Eq. (15), hence the corresponding uncertainties regarding the overall dynamically reconstructed RSS.

VII. Simulations

For the simulations, a SAR model is considered with partially (fractionally) synthesized aperture as an RS imaging system [10], [11]. The SFO is factorized along two axes in the image plane: the azimuth (horizontal axis) and the range (vertical axis). Following the common practically motivated technical considerations [10], [11] a triangular shape of the SAR range ambiguity function of 3 pixels width, and a $|sinc|^2$ shape of the side-looking SAR azimuth ambiguity function of 10 pixels width at the zero crossing level are modelled.

The results of the simulation experiment are indicative of the enhanced quality of SSP and RSS reconstruction with the proposed approach, and are reported for a scene borrowed from the real-world RS imagery of the Metropolitan area of Guadalajara city in Mexico [12].

Fig. 1 shows the original super-high resolution test scene (not observable in the simulation experiment with partially synthesized SAR system model).

Fig. 2 presents the results of SSP imaging with the conventional matched spatial filtering algorithm [1].

Fig. 3 presents the SSP reconstruction applying the proposed RFBR method of Eq. (14).

Fig. 4 presents the HEM extracted using the fused WOS-MDM algorithm, applying the classification operator defined by the Eq. (3). Such HEM is specified as 2-bit 512x512 pixel hydrological RSS that classify the areas in the reconstructed scene images $\hat{B}(\mathbf{x})$ into four classes: areas covered with water (black zones in the figures), the humid areas (heavy-gray zones), the dry areas (light-gray zones), and non classified regions (white zones). The fused WOS-MDM algorithm segments and classifies the RS scene and provides a HEM that is highly-accurate compared with the in-site a priori information model.

Fig. 5 shows the results of the dynamical HEM post-processing for a discrete-time evolution model, obtained with the application of the derived algorithm defined by the Eq. (19). This simulation present the evolution in time of the physical characteristics specified by the HEM displayed in Fig. 4. Darker zones represent the filtered change behaviour of the HEM in its discrete-time evolutions.

The analysis and interpretation of these results require more investigation and are the matter of further studies.

VIII. Conclusions

We have developed and presented the RFBR method for high-resolution SSP estimation and RSS mapping as required for reconstructive RS imagery although it may also be applied to other fields.

The presented simulation examples illustrate the overall imaging performance improvements gained with the proposed approach. The simulation experiment verified that the RSS extracted applying the RFBR reconstruction method provide accurate physical information about the content of the RS scenes.

Also, we have developed the dynamical RSS post-processing scheme that reveals some possible approach toward a new dynamic computational paradigm for high-resolution fused numerical reconstruction and filtration of different RSS maps in evolution time.

The presented study establishes the foundation to assist in understanding the basic theoretical and computational aspects of RS image enhancement, extraction of physical scene characteristics and their dynamical post-processing.

The reported results of simulation study are indicative of a usefulness of the proposed approach for monitoring the physical environmental characteristics, and those could be addressed for different end-user-oriented environmental resource management applications.

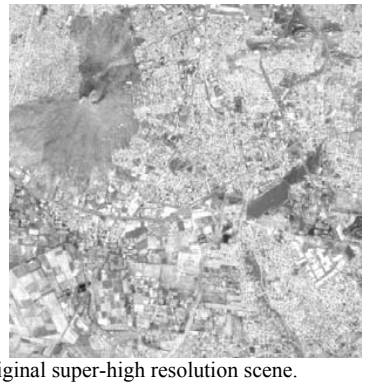

Fig. 1. Original super-high resolution scene.

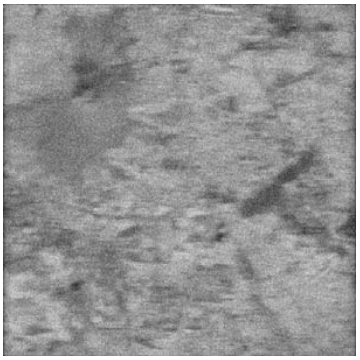

Fig. 2. Low-resolution image formed with the MSF.

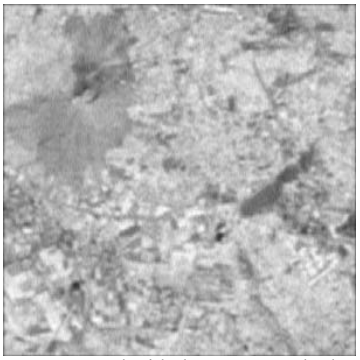

Fig. 3. SSP reconstructed with the RFBR method.

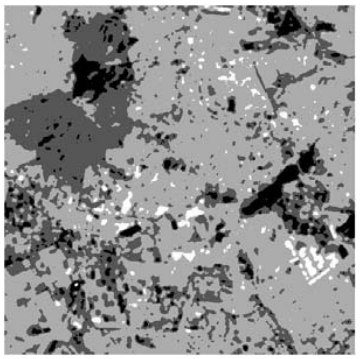

Fig. 4. HEM extracted from the RFBR reconstructed scene applying the fused WOS-MDM method.

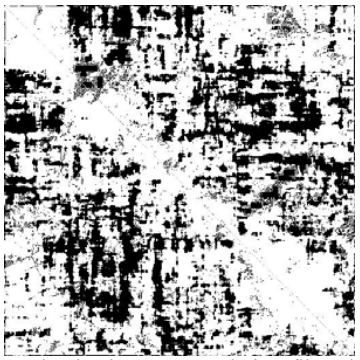

Fig. 5. Dynamics in the HEM evolution filtered from Fig. 4: darker zones represent the areas that have been changed with the evolution.

ACKNOWLEDGEMENT

The author would like to thank the National Council of Science and Technology (CONACYT) of Mexico for the sponsoring of this research by the project number 43290-A and the scholarship number 165660.

REFERENCES

[1] Y.V. Shkvarko, "Estimation of wavefield power distribution in the remotely sensed environment: bayesian maximum entropy approach" *IEEE Transactions on Signal Processing*, vol. 50, pp. 2333-2346, 2002.

[2] Y.V. Shkvarko, "Unifying regularization and bayesian estimation methods for enhanced imaging with remotely sensed data part I – theory" *IEEE Transactions on Geoscience and Remote Sensing*, vol. 42, pp. 923-931, 2004.

[3] Y.V. Shkvarko, "Unifying regularization and bayesian estimation methods for enhanced imaging with remotely sensed data part II – implementation and performance issues" *IEEE Transactions on Geoscience and Remote Sensing*, vol. 42, pp. 932-940, 2004.

[4] B.R. Mahafza, *Radar Systems Analysis and Design Using MATLAB*. CRC Press, 2000.

[5] Y.V. Shkvarko, I.E. Villalon-Turrubiates, "Dynamical enhancement of the large scale remote sensing imagery for decision support in environmental resource management," in *Proceedings of the 18th Information Resource Management Association International Conference*. Vancouver, Canada: Idea Group Inc., 2007, in press.

[6] S.W. Perry, S.W, H.S. Wong and L. Guan, *Adaptive Image Processing: A Computational Intelligence Perspective*. CRC Press, 2002.

[7] J.R. Jensen, *Introductory Digital Image Processing: A Remote Sensing Perspective*. Pearson, 2005.

[8] S.E. Falkovich, V.I. Ponomaryov and Y.V. Shkvarko, *Optimal Reception of Space-Time Signals in Channels with Scattering*. Radio I Sviaz, 1989.

[9] I.E. Villalon-Turrubiates, "Intelligent processing for SAR imagery for environmental management," *in Proceedings of the 19th Information Resource Management Association International Conference.* Washington D.C., USA: Idea Group Inc., 2006, pp. 981-983.

[10] F.M. Henderson and A.V. Lewis, *Principles and Applications of Imaging Radar*, ser. Manual of Remote Sensing. Wiley, 1998.

[11] D.R. Wehner, *High-Resolution Radar*. Artech House, 1994.

[12] Space Imaging, *http://www.spaceimaging.com/quicklook*. GeoEye Inc., 2007.